Just Keep Swimming?

Understanding the Effects of Climate Shifts through Observations of Fish Productivity in the Southern Pacific Ocean across the Eocene-Oligocene Boundary (IODP Site U1553)

Iszac M. Henig

Advised by: Dr. Elizabeth Sibert and Dr. Pincelli Hull

Read by: Dr. Pincelli Hull and Dr. Derek Briggs

28 April 2023

A Senior Thesis presented to the faculty of the Department of Geology and Geophysics, Yale University, in partial fulfillment of the Bachelor's Degree.

Contents

Abstract

The planet is currently undergoing a large shift in climate, which has effects on global ocean temperatures, ice volume, and circulation, which in turn affect organisms that have evolved to survive under certain conditions. Increased understanding of the effects of previous climate shifts on ecosystems can help us understand the sensitivity to modern anthropogenic (climate) changes. Across the Eocene-Oligocene Transition (EOT), a period of time beginning just before and ending just after the E-O boundary (EOB) at 33.9 million years ago (Ma), the globe underwent significant changes, with cooler temperatures, the rapid growth of Antarctic ice, and initiation of global ocean circulation patterns similar to those observed today. These shifts had implications for marine and terrestrial organisms[1]. This thesis is focused around data from International Ocean Discovery Program (IODP) Site U1553, where pelagic fish populations experienced shifts throughout the interval, as calculated by ichthyolith accumulate rate (IAR). Fish populations declined throughout the late Eocene, in line with cooling water and ice growth, but experienced a sharp rebound in the Early Oligocene after minimum temperatures and maximum ice extent were reached. The preliminary results show no major transition in fish productivity at Site U1553 between the late Eocene and Early Oligocene. These observations are distinct from other sites that have been analyzed using the same methods across the EOT, which may be due to local conditions at Site U1553, which may have had stronger effects than the globally-observed shifts. The initial results from Site U1553 contribute to a greater understanding of how much changes in local conditions impact population dynamics in contrast to –or in combination with– significant global climate shifts.

Introduction

Across the EOT, Earth's climate switched from the previous, early Cenozoic 'greenhouse' state to the modern 'icehouse' state. The 'icehouse' state is marked by the permanent glaciation of Antarctica and cooler land and sea-surface temperatures across high-, middle-, and low-latitudes[2,3]. This change occurred relatively quickly, with cooling of up to 3 to 5°C in deepwater[4] and a cooling of annual mean land temperatures by 4 to 6°C[5] occurring across less than half a million years, and much of the ice growth occurring across 50,000 years[6]. Rapid, large-scale shifts in climate, such as the one observed at the EOT, have strong implications for organisms accustomed to specific ranges of temperatures or other environmental conditions. The EOT is considered a major extinction event all over the globe, with established evidence from terrestrial ecosystems [7–13]. Increasing our understanding of how marine organisms are affected by global climate shifts in temperature and circulation lends insights that could be applied to modern-day global warming.

Data gathered from IODP Site U1553, at the same location as Deep Sea Drilling Project (DSDP) Site 277, situated off the southern coast of New Zealand at approximately 52°S, 166°E and 1220m water depth[14], provides insight into the effects of global glaciation in the high-latitude of the Southwestern Pacific Ocean. The historic DSDP 277 site, a single core drilled in 1973, provides information to compare with the new findings from this thesis. The location is characterized by its proximity to land and the presence of cold water upwelling, which is thought to have increased across the EOT with increased circulation[15–17]. These factors suggest elevated primary productivity at IODP Site U1553/DSDP Site 277 compared to open-ocean sites due to increased nutrient cycling. Increased primary productivity is usually associated with increased secondary (consumer) productivity, which can be measured in part as increased fish biomass.

Records of fish biomass at the EOT can be approximated through the record of ichthyoliths (fish teeth, shark scales, and other fish bone fragments) accumulating in sea floor sediments through time.

Pelagic marine ecosystems are a vital component of global productivity. Observing the impacts on historic pelagic fish populations across the EOT helps to expand the understanding of the sensitivity of marine life in the face of modern climate change. Terrestrial ecosystems also experienced significant changes with the extinction of many warm-climate-adapted species and a notable dominance of cold-climate-adapted species across the globe[1]. Incorporating comparisons of the sensitivity of marine ecosystems to these changes with the sensitivity of local and global terrestrial ecosystems helps increase understanding of the broader effects of climate change.

Motivations

Fish, as secondary consumers that respond to a variety of factors, can be an important indicator for ecosystem health[18,19] including sensitivity to temperature, salinity, nutrient concentrations, and plankton communities, among others. Additionally, in a near-coast environment, the response of fish populations to large climatic shifts is relevant for human subsistence. Globally, fisheries produce over 179 million tons of marine organisms for consumption, a number that increases as aquaculture becomes more prominent[20]. Existing and future changes to marine ecosystems and fish populations are highly relevant to the 600 million people worldwide living within 10 km of the coast, and especially to those in the more than 260 million fishery jobs[21]. Reliance on fish for subsistence is a global issue, with poorer countries, especially the global South, confronting higher food insecurity as fish populations struggle with climate change[20,22]. Observing patterns of fish population responses to changes in temperature

and ice growth can provide insights into how sensitive modern fish populations are to changes that could occur.

It is important to note that the modern climate trend involves rapid warming, where the EOT was characterized by cooling. Thus, the exact effects of the EOT on pelagic fish populations should not be understood as a parallel to the modern but as a helpful insight into the fragility and responsiveness of marine ecosystems to rapid climatic shifts.

Background

The E-O Boundary

The Eocene-Oligocene transition is notable for the establishment of the Antarctic ice sheet[23], rapid global cooling[4,5,24–26], and extinction events worldwide. While early papers placed the E-O boundary at anywhere between 40 and 32 Million years ago (Ma)[27], it is now generally accepted to fall around 33.9 Ma[28,29]. The E-O boundary is marked at the base by the extinction of marine foraminifera, providing a standard nannofossil marker (*D. saipanensis*) globally[1]. Between 33 and 34 Ma, global sea temperatures decreased by 5°C on average at high latitudes (45 to 70°)[4] and approximately 2.5°C on average globally[2]. High latitude deep sea temperatures decreased between 2-3°C[24] while sea surface temperatures (SST) may have decreased by up to 6°C[3]. There is also a decrease in atmospheric CO_2 across the Oligocene to near-modern levels (approx. 400 ppm) from 1000-1500 ppm in the Eocene[30], a trend that is consistent with a gradual decline in atmospheric CO_2 throughout the Cenozoic[31].

These temperature changes are evidenced by three well-documented proxies for conditions at the EOT: oxygen-18 isotope fractionation in marine calcite ($\delta^{18}O$), Mg/Ca ratios, and the TEX_{86} proxy (outlined in [32]). O^{18} is excluded in ice formation and seawater oxygen

capacity increases with lowered temperature. Thus, $\delta^{18}O$ is used as a proxy for both ice growth and water temperature[1], and the EOT is marked by a sharp increase in deep-sea $\delta^{18}O$ content by more than 1.0‰[31]. It can often be difficult to separate the effects of ice growth versus temperature drop, which is why it is helpful to examine the changes through other proxies, as well. Mg/Ca ratio calculations also serve as a proxy for temperature, recording drops in water temperature, although less extreme than those suggested by the $\delta^{18}O$ record[24,25]. Mg/Ca ratios are used in combination with $\delta^{18}O$ in order to isolate the effects of temperature from ice growth and to correct for the sensitivity of Mg/Ca ratios to changes in deep-water carbonate ion concentration[24]. The TEX_{86} proxy relies on measurements of lipid membranes of marine plankton (*Crenarchaeota*) to reconstruct sea surface temperature[32], and contributes to a robust established trend of ocean temperature drop across the Eocene[3]. When coordinated, all three proxies point to cooling across the EOT.

A fourth proxy, clumped isotope (Δ_{47}) thermometry, offers a model of temperature unaffected by seawater pH, temperature changes, or physiological uptake differences across species, as the $\delta^{18}O$ and Mg/Ca proxies are. Clumped isotope thermometry involves examining the ordering of isotopes within molecules in order to model temperature, with results suggesting deep ocean temperatures globally were likely warmer by about 3 to 5°C in the late Eocene than previously modeled by $\delta^{18}O$ due to the influence of ice growth on $\delta^{18}O$. Still, a decrease of up to 4°C in North Atlantic deep ocean temperature is observed in the Δ_{47} reconstruction[33], which appears to be consistent with other proxy data.
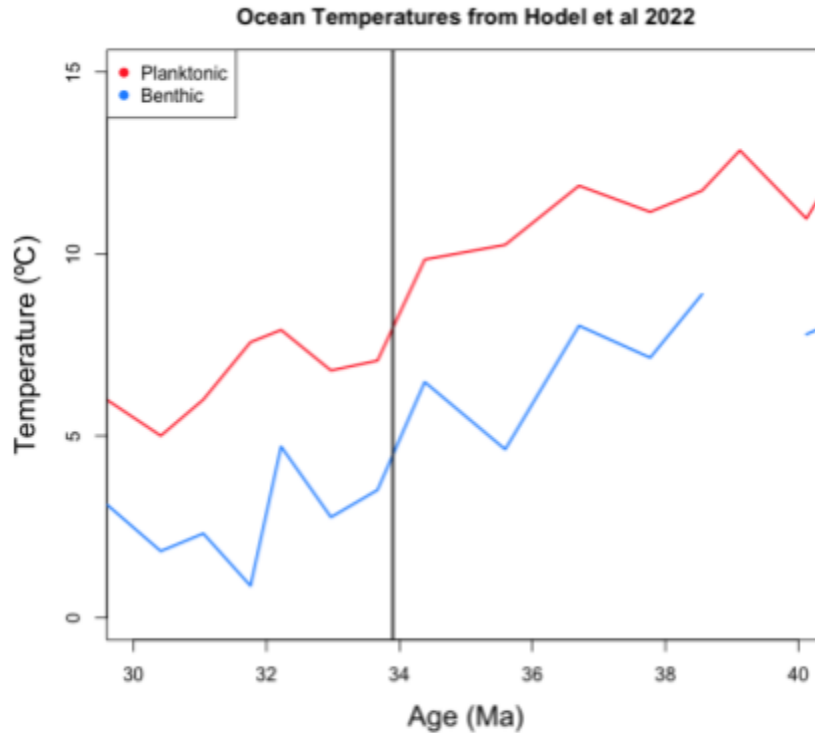
Figure 1: Ocean temperatures at DSDP Site 277 from Hodel et al. (2022) [25] from Mg/Ca ratios from planktonic (red) and benthic (blue) foraminifera (*Subbotina*).

The mechanism behind the EOT rapid cooling and Oligocene growth of the ice sheets has been poorly understood, with many competing theories about what happened. Leading modern theories behind the growth of the Antarctic ice sheet include decreased atmospheric carbon dioxide (CO_2) concentrations[31] and, secondarily, the opening of Southern ocean circulation through natural tectonic shifts[17,31]. Through time many theories have been posited, including, at one point, a theory that an asteroid impact caused the extinctions observed at the EOT[34] (largely inspired by the discovery of the impact mechanism behind the K-Pg mass extinction two years prior[35], but that was soon disproved[36] and abandoned.

One observed mechanism that may relate to the cooling of ocean bottom water is the linked suppression of the Iceland mantle plume, a rift feature that generates thicker-than-average oceanic crust, and the deepening of the Greenland-Scotland Ridge (GSR), a ridge of oceanic

crust which traces the plume[15]. A deepening of the GSR would have allowed for the initiation of the observed, modern-day patterns of deepwater formation in the North Atlantic (NADW) which then flows into the Atlantic. This global deep-ocean circulation exerts important climatic controls, which could have included stabilizing the cooler climate required for sustained Antarctic glaciation[16].

Across the EOT, the hypothesized increase in deepwater circulation is matched by an observed split between $\delta^{18}O$ values for planktonic foraminifera as compared to benthic values, implying greater ocean temperature stratification[15]. Increased circulation of NADW, and therefore lowered ocean bottom water temperatures globally could have contributed to lowered carbon dioxide concentrations via an increase in carbon dioxide absorption[37]. All of the evidence points to important near-simultaneous changes in ocean circulation, a continued decrease in atmospheric CO_2, and decreased temperatures across the globe around the EOT.

IODP Site U1553/DSDP 277 Conditions

The global changes across the EOT had significant effects on the local conditions at the site. Local sea level may have fallen by up to 70m[38], associated with the growth of the Antarctic ice sheet). $\delta^{18}O$ records show a two-step decrease between 33 and 34 Ma. The second step, around 33.2 to 33.6 Ma, is interpreted as the onset of a period of maximal Antarctic ice extent, known as the Earliest Oligocene Glacial Maximum (EOGM), attributed to a decrease below 600 ppm of atmospheric CO_2[39].

According to the TEX_{86} proxy, minimum sea surface temperatures at Site 277 may have been reached at 33.5 Ma, with a drop from around 27°C pre-EOT to around 23°C[4]. Interestingly, Mg/Ca ratios indicate that local mixed-layer temperatures remained somewhat stable across the

EOT but appear to have fallen sharply (from ~22 to 20°C) just before, beginning around 37 Ma[25].

An $\delta^{18}O$ analysis conducted in the same study indicates a 4 to 5°C drop in seafloor temperatures

across the interval[25]. This observation could be due to the use of Mg/Ca ratios from planktonic

foraminifera, which tend to report less extreme temperature fluctuations compared with $\delta^{18}O$.

While there is some disagreement between the metrics, it is clear that there were significant

decreases in both sea surface and seafloor temperatures around the interval.

Southern ocean circulation increased with the opening of Southern Ocean gateways such

as Drake's Passage and the Tasmanian Gateway[17,31]. Drake's Passage, the flow between

Antarctica and South America, is a key component of the Meridional Overturning Circulation

(MOC) which links surface water in the Southern Ocean with NADW formation[17]. The

Tasmanian Gateway between Australia and Antarctica is another key opening that would have

'thermally isolated' Antarctica by eliminating the land connection thereby establishing the

Antarctic Circumpolar Current (ACC) and reducing ocean heat transport to southern waters[17,31].

These openings would have cooled Southern Ocean waters and increased surface flows which

would increase upwelling locally at Site U1553[40,41].

Extinctions Across the EOT

The EOB is identifiable in marine settings due to the extinctions of many foraminifera

and echinoid species[7] as well as high marine turnover rates including a 90% turnover rate for

mollusc species in the US Gulf coastal plain[8]. Proposed mechanisms for extinction include

decreased ocean temperatures both at the surface and at depth[4,25] but also an increase in

seasonality and colder winters[8].

The climatic shift is recognizable on land, as well. Global cooling and decreased CO_2 content had significant effects on terrestrial organisms: the EOT is the most recent recognized major global extinction event, showing a 15.6% proportion of genus loss[7]. However, the effects were not felt equally across the globe.

In Europe, the transition is known as the "Grande Coupre" or "Great Break", when large endemic herbivores were largely replaced by immigrant species[9]. Insectivores and primates were also less abundant in Europe in the Oligocene than in the Eocene[42]. In Asia, the period is referred to as "Mongolian Remodelling", showing a large turnover in fauna from warm, humidity-favoring morphologies to cool, arid-favoring ones, matching the expectations with the posited climate shift. This trend is also reflected in body size: there is a shift away from larger mammals towards smaller rodents and lagomorphs (rabbits and hares)[10,11]. In North America, species origination in the early Oligocene is 43% lower than the mean from the last 55 million years[12]. North African primate records show a slow decline across the Eocene and through the Oligocene, but no major extinction event right at the boundary[13].

The observed extinctions were likely climate-driven, with cooling observed across many parts of the globe. In North America, continental annual mean temperatures may have dropped close to 8°C across a period of 400,000 years around the EOT[26]. Mammalian turnover (specifically replacement of *Perissodactyla* by rodents and lagomorphs) in Asia is linked to both cooling and aridification[43,44]. These records are important to understand the links between marine and terrestrial events and the global implications of large climatic shifts on different kinds of ecosystems. The observed cooling (global) and regional (Asian subcontinent) aridification across the EOT may be linked to changes in heat transport and rainfall patterns, which are informed by global oceans[45].

Marine Productivity & Ichthyoliths

Productivity, or the amount of biologically fixed carbon, is a structural characteristic of marine ecosystems. The amount and type of production at the base of the food web can drive changes to the biodiversity and biomass of organisms across the web. Primary (base) productivity in marine ecosystems is mainly controlled by phytoplankton, in a relatively closed loop that cycles nutrients in the surface waters. Secondary (consumer) productivity is particularly sensitive to "new" nutrient inputs, such as from upwelling and mixing[46]. The Eocene-Oligocene transition has been associated with an increase in overall productivity, especially silicate organism primary production[47]. Previous studies focused on foraminifera or diatoms as proxies found increases in productivity, as evidenced by silicon isotope ratios[48] and foraminiferal accumulation rates and carbon isotope analysis[41] with upticks attributed to favorable changes in ocean currents and upwelling[41,48]. As fish are dependent on primary production transferring up the food web, it is likely that increases in productivity recorded in diatoms and foraminifera would also be reflected in fish populations.

Fish biomass can be approximated from ichthyoliths, isolated microfossil fish teeth and shark scales found in marine sediments. Ichthyoliths preserve information about the marine ecosystem at the time, including serving as a means for quantifying changes in fish biomass and tracking different morphologies associated with different feeding techniques.

Changes in primary productivity mean changes in availability and type of food available to fish populations, making fish biomass sensitive to changes in primary productivity. Tracking changes in primary production and fish populations generates information about potential changes in higher-level consumers, like early species of whales and sharks[49]. Alongside the fish

teeth, shark scales (denticles) are preserved. Those denticles, while rarer in the sediments, can provide information about shark biomass changes during this period.

In this thesis, I explore the effects of the changing climate across the Eocene-Oligocene Transition by counting and analyzing ichthyoliths (fish teeth and shark scales). The data is analyzed on its own as well as in conversation with previous datasets. It joins a larger collection of sites analyzed using similar methods across the same time period, bringing the number to 8 sites globally[50].
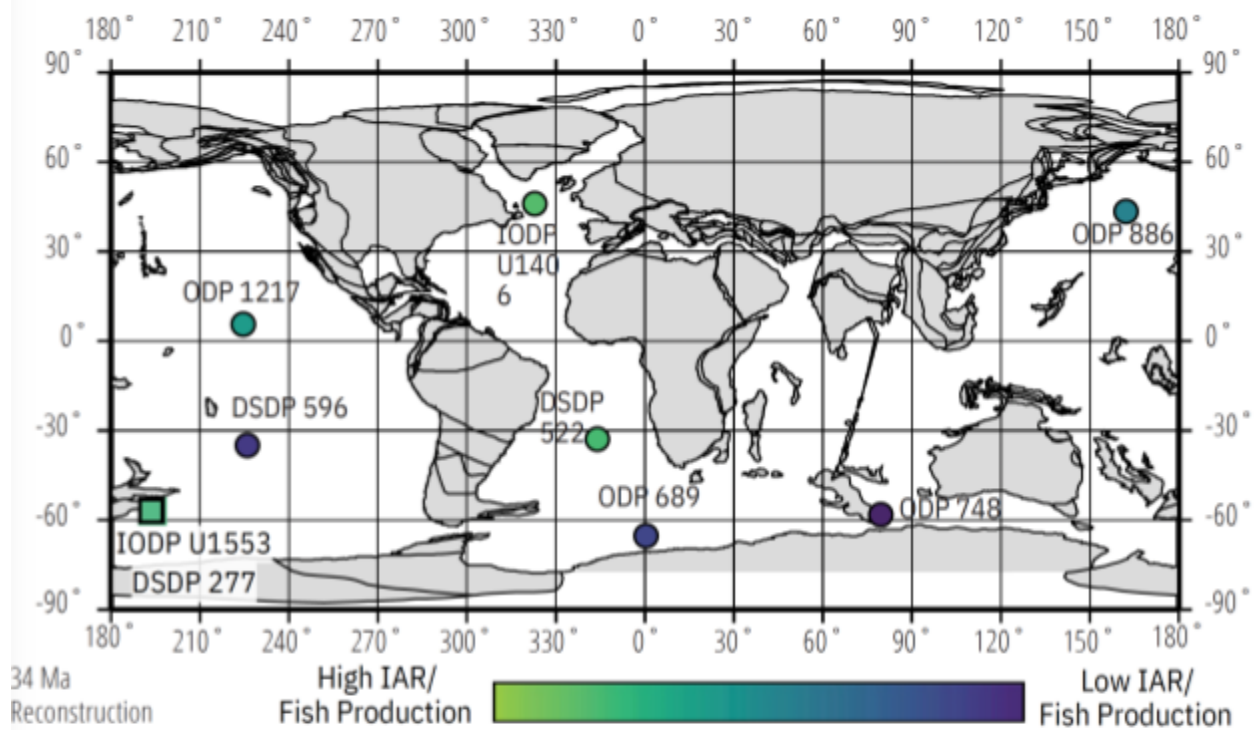
Figure 2: IODP Site U1553 joins other existing datasets, mapped here on a reconstruction of continents during the Eocene-Oligocene[50]. The productivity of Site U1553 is on the higher end of global fish productivity, as noted by the green color.

Methods

The data collected in this project relied entirely on the ability to isolate, count, and image ichthyoliths from the sediments at IODP Site U1553. The methods applied for this data collection align with and attempt to optimize the methods outlined in Sibert et al. 2017([51]). The methods were refined throughout the project in order to maximize isolation and concentration of ichthyoliths while minimizing potential loss of valuable data. For time efficiency, several samples were brought through the stages in parallel.

Sample Processing

To begin processing, samples were dried to constant weight in a 50°C oven then put into sodium metaphosphate, a disaggregating agent. After 1-3 hours, the disaggregated samples were washed through a fine, 38μm sieve until all particulate matter smaller than 38 μm was removed, typically around an hour to two hours of washing. Samples were then dried overnight and, if necessary, disaggregated, washed, and dried again. Dry samples were then separated using a dry sieve at 150μm. The fraction larger than 150μm was retained for other uses, as there were few preserved ichthyoliths in this fraction. The <150μm fraction was put into a 5-10% acetic acid (CH_3COOH) solution for 2 to 6 hours, dissolving most of the carbonate material, eliminating the amount of sediment to be 'picked' through. Acidification was followed by a second, shorter rinse and another overnight dry.

The sediment samples processed and analyzed in this study were particularly silica-rich, necessitating the inclusion of a heavy liquid separation step, which relies on LST, a low-toxicity heavy liquid with a density of 2.8 $g/cm^{3,52}$. Samples were left in LST overnight to separate. The silicate 'floats' (density 2.3-2.6 g/cm^3) were collected off the top of the LST and the 'sinks',

consisting of apatite (density 3.1 g/cm$_3$) and other dense materials, were collected for picking. Removing the silicate material, which accounted for more than 90% of the sample volume, minimized the amount of sediment to be looked through. After separation, the floats and sinks were washed separately; the floats, which have no remaining ichthyoliths, were retained for other uses. Once dried, the sinks were separated via dry sieve into three size fractions: 38-63μm ("Small"), 63-106μm ("Medium"), and 106-150μm ("Large"). These fractions were then picked in sequence, large to small.
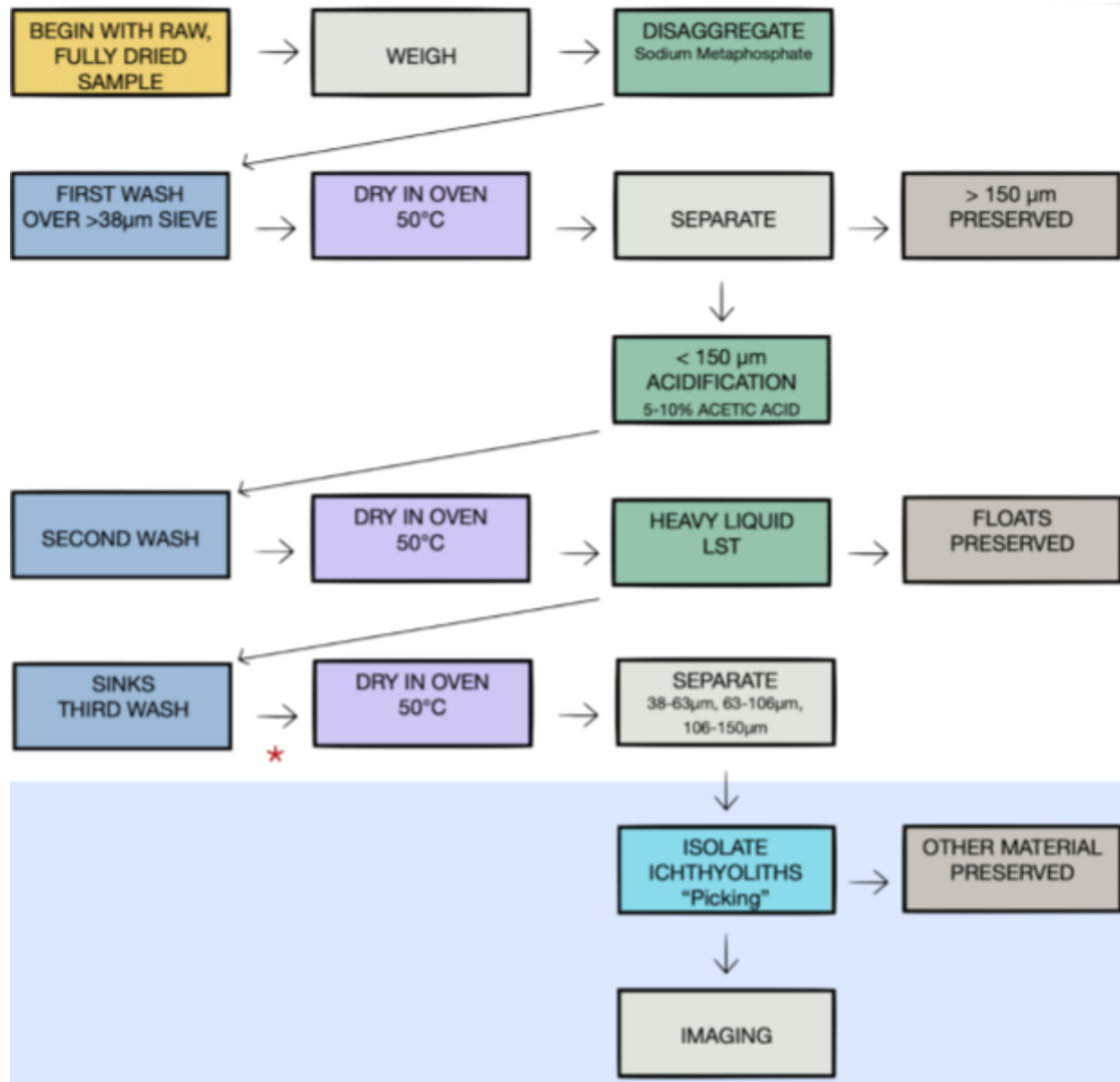
Figure 3: This Methods Flowchart visualizes the various steps involved in processing and data collection. Blue background denotes the data collection stage. *The red asterisk denotes where, for one sample (#33), a staining step was added to processing. Apatite material was identified using Alizarin Red S, in order to speed up the data collection process. This ultimately had a minimal effect on picking, but slowed down processing by a full day and introduced the possibility of loss due to another wash, so was abandoned.

Picking

     Picking is the process by which ichthyoliths are isolated and removed from the remaining sediment via two high-power microscopes and fine paintbrush. Ichthyoliths are moved from the tray containing the sample sediment (left) to a four-hole slide (right). The four hole slide is coated with a water-soluble glue before picking begins to ensure that isolated ichthyoliths are not lost once isolated.

Figure 4: Double microscope picking set-up

     Once picking has been completed, the four-hole slide can be imaged using a high-powered imaging microscope. In this case a Keyence VHX-7100 digital microscope system was used. These images (Fig. 5) can be analyzed for morphological data.
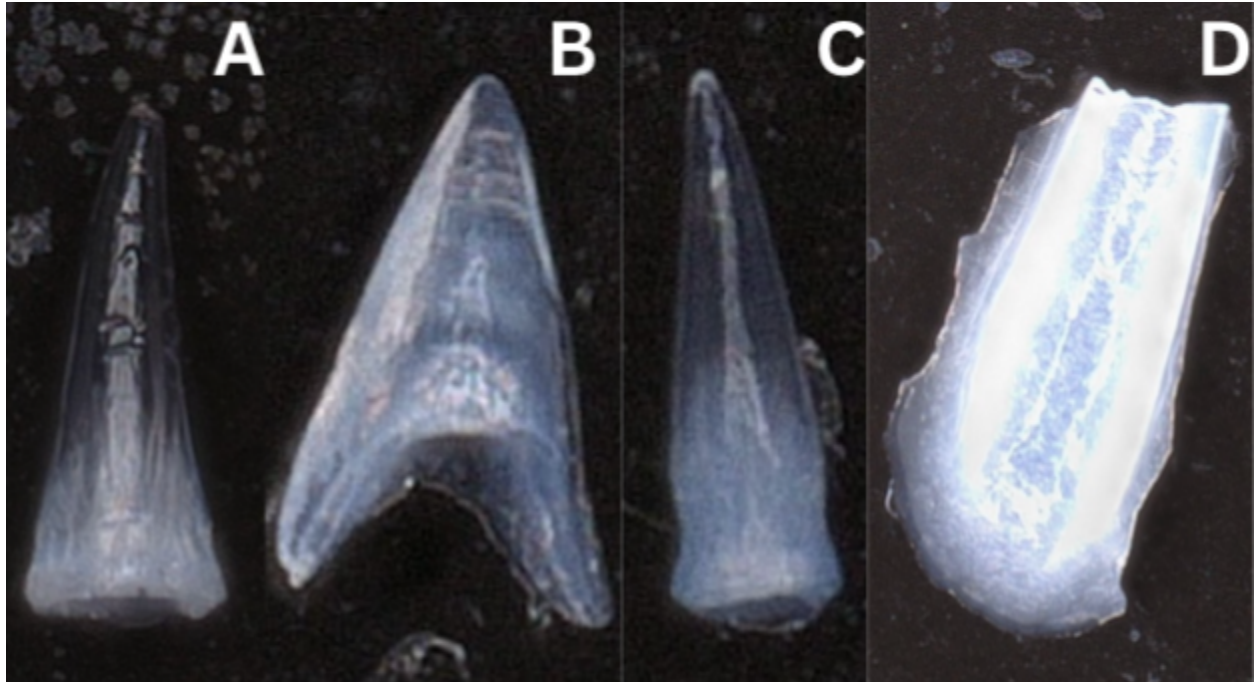
Figure 5: Images taken by the Keyence VHX-7100 of fish teeth (A, B, C) and a denticle (shark scale) fragment (D). Sizes not to scale relative to one another; magnified to show texture.

Minimizing Loss

Data can be lost in each of the stages of processing, in different ways. Ichthyoliths, which are both extremely small and sensitive to static cling, can stick to various surfaces including vials, sieves, paintbrushes, and beakers. Steps, detailed below, were taken to mitigate the leaving behind of any sample in transfer between containers and across processing steps.

During the washing stages, data can be lost as ichthyoliths get stuck in the mesh of the sieve or splashed out. Techniques were used to minimize this loss including using gentler water flows and 'washing up the back' of the sieve after the main portion of the remaining sample has been transferred out of the sieve to unstick teeth that had entered the sieve point-side down. Sieve clearing and rinsing steps were repeated multiple times per sample, to ensure all particles were removed prior to moving to the next sample, and sieves were placed in an ultrasonic bath

for 5-10 minutes between samples to prevent cross-contamination. During the size fraction separation stages, which rely on dry sieves, similar loss can occur with ichthyoliths stuck in the mesh. Additionally, if too much force is used, ichthyoliths can fragment, resulting in a loss of data. During the acidification stage steps are taken to avoid destruction via dissolution. Ichthyoliths are composed of calcium phosphate, also known as bio-apatite, which is resistant to dissolution[51], and samples were never left in acid for more than 6 hours - thus loss due to acid dissolution is relatively unlikely, but nonetheless could contribute to a small amount of sample loss. During the heavy liquid (LST) stage, one initial issue was crystallization of the solution, trapping sediment and interfering with the separation process. This was due to extremely low and fluctuating air temperatures (<15°C) in the lab, and was eventually resolved by placing the separation tubes in a 25.6°C water bath to maintain constant temperature and LST liquid density throughout the separation process. During the picking process some quantifiable loss can occur if ichthyoliths are lost in transfer between slides - when an ichthyolith was lost, it was noted in the processing log for that sample, accounting for a loss of 9 ichthyoliths across all samples in this study.

In order to minimize the impact of error or loss on the final dataset, samples were processed in a random order. This ensured that if, for example, the heavy liquid step crystallized more than expected, making data retrieval difficult, no one batch of lost data interrupted the dataset as a whole. Two samples that were started, #51 (U1553B-23X-2W, 23-29 cm) and #59 (U1553E-26X-3W, 80-86 cm), were impacted by significant errors with processing. #51 was not separated prior to acidification, resulting in loss of carbonates and issues processing the large size fraction. #59 was improperly washed, with data loss occurring through a spill over the edge of a sieve. Neither were included in the final dataset.

Calculations: Ichthyolith Accumulation Rate

Once collected, the raw counts are standardized, to account for varying time intervals and sedimentation rates, through the calculation of an Ichthyolith Accumulation Rate (IAR, ich/cm²/myr) for each sample, described in Equation 1.

1. $IAR\ [ich/cm2/myr]$: $ichthyoliths\ [ich]\ \times\ sedimentation\ rate\ [\frac{cm}{Myr}]\ \times\ dry\ bulk\ density\ (DBD)\ [\frac{g}{cm^3}]$

Sample ages and densities were extrapolated via ship-board models[14]. IAR provides a basis for which to compare across individual samples and to existing ichthyolith data across the globe by ensuring that the values reflect standardized units of production over a given area and period of time.

Results

Both raw ichthyolith count and IAR indicate that fish populations appear to decline throughout the late Eocene from 38 to 34 Ma, reaching a low around 33.7 Ma, just after the EOT. This late Eocene decline in fish abundance mirrors a decline in SST at Site 277[4,25], which reached a minimum around 33.5 Ma[4]. This correlation between IAR-inferred fish abundance and ocean temperature in the Late Eocene at Site 277 is similar to the correlation between bottom water temperature and fish abundance observed at DSDP Site 596 in the Early-Middle Eocene[53]. The Earliest Oligocene, from 33-30 Ma, is marked by relatively elevated IAR with levels similar to the Late Eocene at Site U1553. The preliminary results show no major step-change in fish productivity between the Late Eocene and Early Oligocene, though there may be a brief depression in fish abundance leading up to the EOT.

Throughout the study interval, calculated IAR and the number of counted ichthyoliths (per gram of dry sediment) appear to follow similar trends, which is expected, with a notable exception at around 38 Ma. IAR is strongly influenced by sedimentation rate, which was higher during the middle Eocene and declined into the later Eocene at Site U1553 and could explain that divergence.
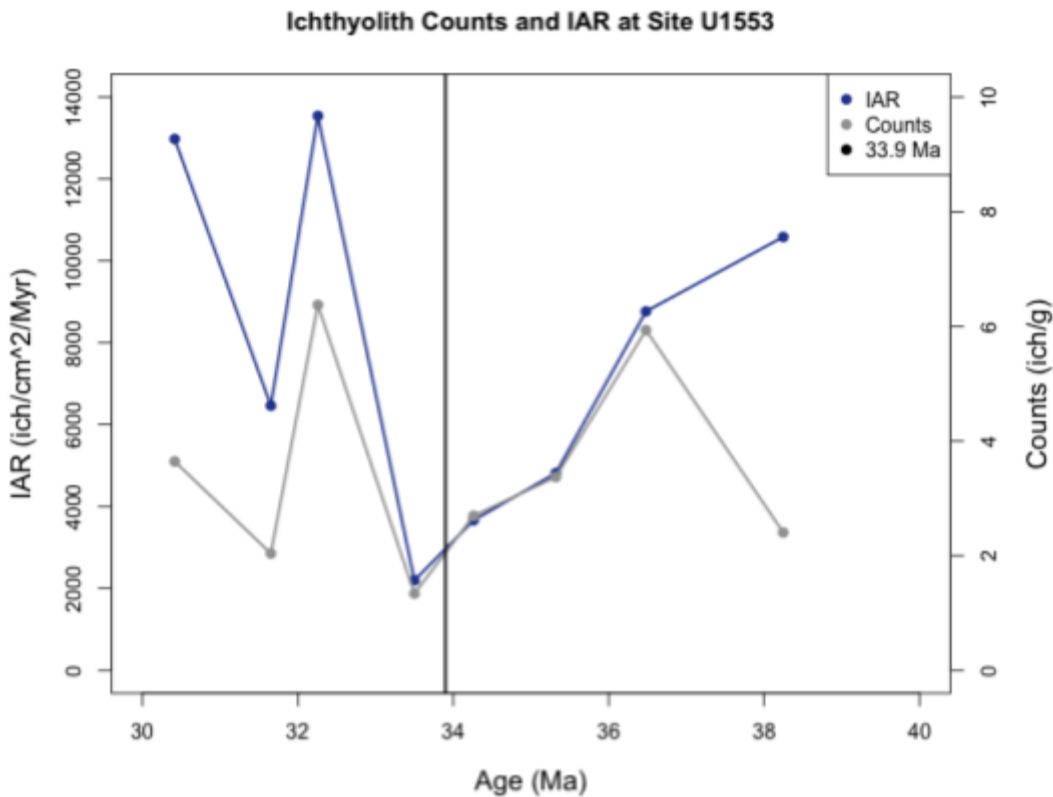
Ichthyolith Counts and IAR at Site U1553

Figure 6: Calculated IAR (ich/cm²/Myr) for each sample (dark blue) and ichthyolith counts per gram of dry sediment (grey) with the Eocene-Oligocene Boundary (EOB) at 33.9 Ma shown with a black vertical line.

Following the EOT, IAR returned to late Eocene levels, suggesting a rebound in fish populations, perhaps due to adaptation to the influences that caused the original decline. This could also mean a switch from a temperature-controlled ecosystem to a different control, like salinity or nutrient content, which could be explored by observing changes in fish size distributions and fish biodiversity.

Ichthyoliths are not evenly distributed across the various size fractions: the majority of the teeth (63% on average) came from the smallest size fraction (38 to 63μm). The opposite is true for denticles, where the majority (80%) are found in the largest size fraction (106 to 150μm). There is less variability in counted denticles - and inferred shark populations - however there are

very few (10 preserved denticles compared to 1214 preserved teeth) in these 8 samples and it is

impossible to draw any robust conclusions about shark populations across the EOT at this

location.

In order to investigate any trends in fish size, ichthyolith accumulation rates were

calculated across the various size fractions. The large size fraction appears to experience a small

increase just before the EOT, countering the trends in the medium and small size fractions which

continue to decline. The larger size fraction has less variability across the entire interval, but

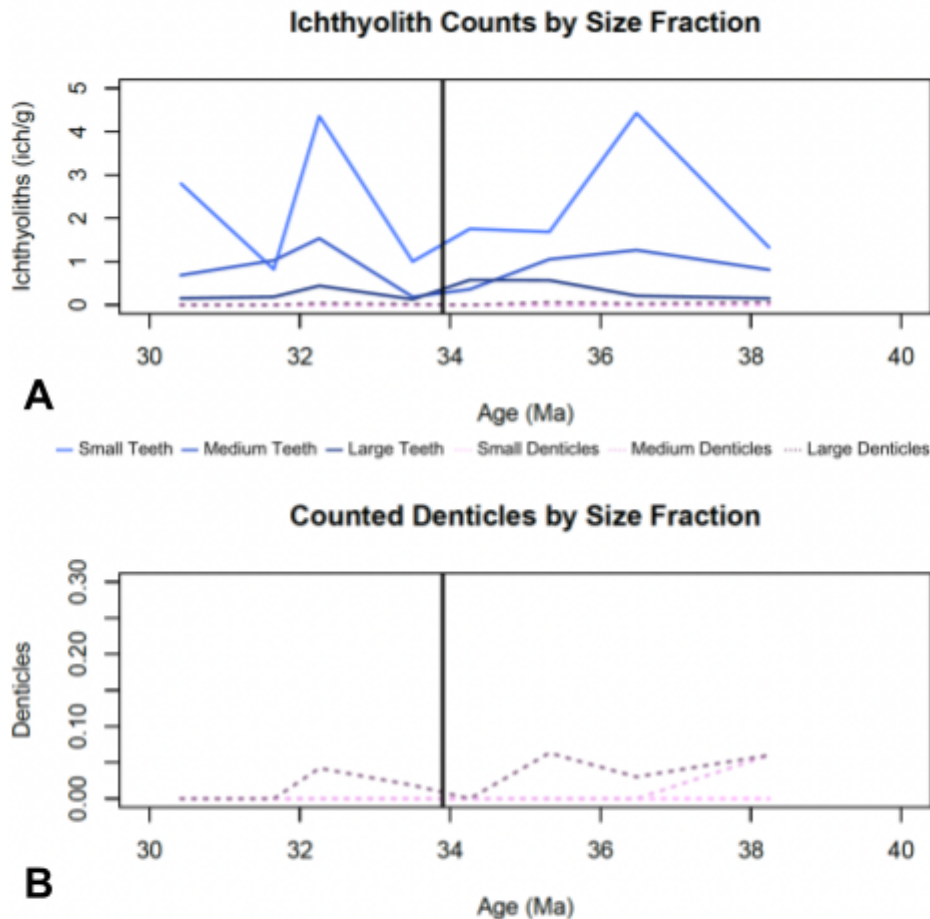there are fewer ichthyoliths in that fraction in general.

Figure 7: A. Ichthyolith counts (ich/g) by size fraction, shown in blue (dark to light from large to small) solid lines and B. Denticle counts (dents/g) by size fraction shown in pink (dark to light from large to small) dotted lines. EOB shown in black.

There is no apparent change in the size structure of the fish community across the EOT, and the proportions of fish size seems to remain unchanged. However, there are relatively few samples in this dataset, so trends in fish size may be illuminated with more samples across the time interval.
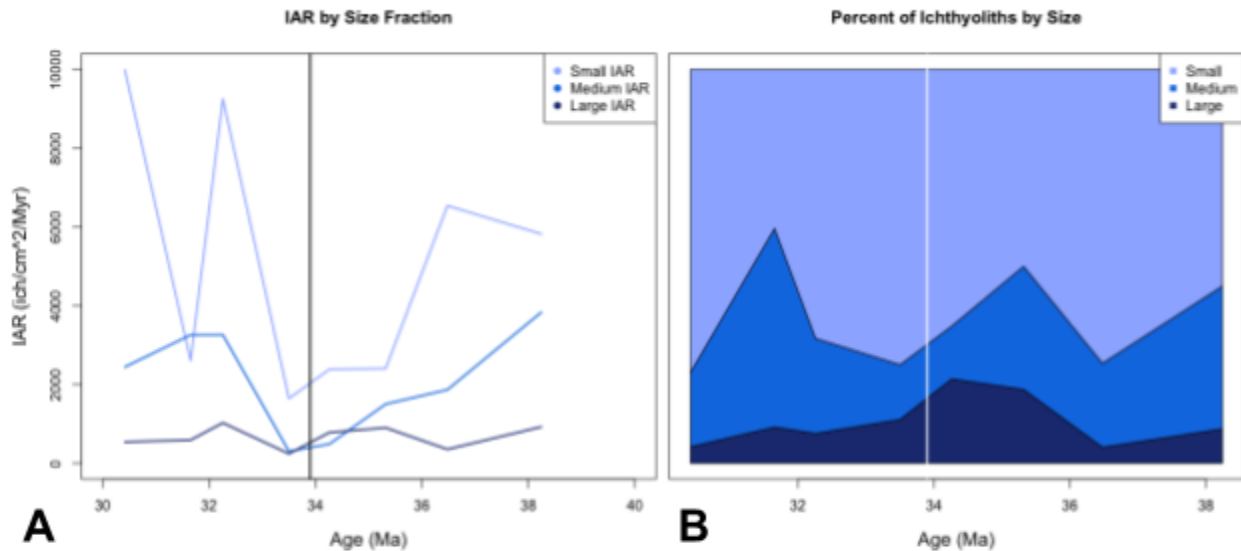

Figure 8: A. IAR by size fraction, with EOB shown in black B. Percents of ichthyoliths by size fraction, with EOB shown in white. For both, size fractions are shown in blue, light to dark from small to large

Discussion

Local Environmental Changes at Site U1553

The patterns observed at Site U1553 match the global trend over the interval in that pelagic fish populations do not seem to experience permanent population changes across the EOT. Effects vary largely based on local conditions, such as local temperature, ice volume, and circulation patterns.

A multi-proxy record from DSDP Site 277, including Mg/Ca, $\delta^{18}O$, and TEX_{86} reconstructions, shows a decline in sea surface temperature throughout the EOT from [40-30 Ma]

(Figure 9). During the late Eocene, fish abundance declines alongside temperature, however IAR becomes decoupled from temperature in the Oligocene, returning to middle Eocene levels by approximately 31 Ma[25].
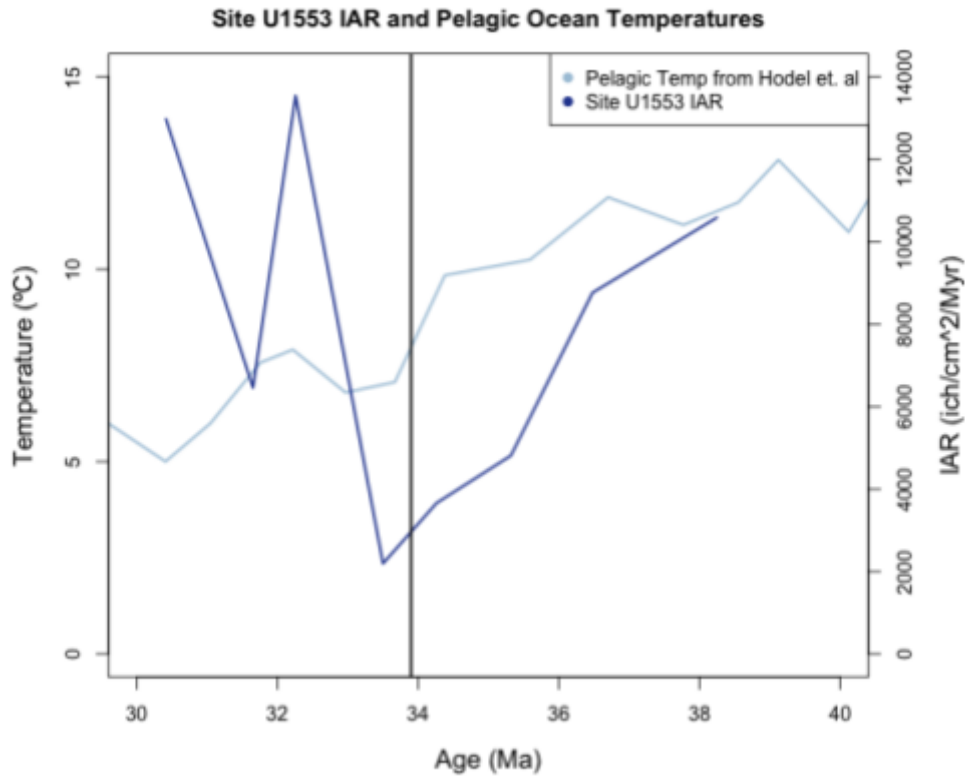

Figure 9: IAR (ich/cm²/Myr) from this thesis plotted against pelagic temperatures (°C)[25]

One potential explanation for this is adaptation of fish populations to new or more variable conditions. Sea surface temperatures began decreasing through the middle Eocene[54], but as temperatures decreased more rapidly in the later Eocene, stress on fish populations may have increased and led to decline. However, the effects of decreased temperature are not necessarily opposite to increased fish biomass. Decreased temperature means increased oxygen content, increasing the capacity for phytoplankton, increasing fish populations through eventual predation. This mechanism may be responsible for the apparent rebound after the EOT.

Ice growth across the EOT would have lowered sea levels and changed circulation patterns. Sea level changes at the EOT were on the order of 70 meters, and are unlikely to have had a direct effect on fish populations around Site U1553, which is thought to have had similar water depths at the EOT to today (>1000m)[55]. However, sea level records are a useful record of ice volume growth, and changes in sea level may have impacted nutrient run-off from the coast to Site U1553.

The maximum sea ice extent (lowest sea level) and lowest observed instance of fish productivity appear to align temporally. This seems to suggest that, at Site U1553, ice growth is in part correlated with the decline of fish populations at Site U1553 before the EOT. This may again be explained by greater stress on local ecosystems and then their eventual adaptation as well as a potential shift in ocean currents and a decrease in upwelling, limiting nutrient availability. Beyond the changes to overall fish biomass, the changes observed in the distribution of large, medium, and small teeth (plotted in Fig. 8) may be due to changes in food source and temperature.
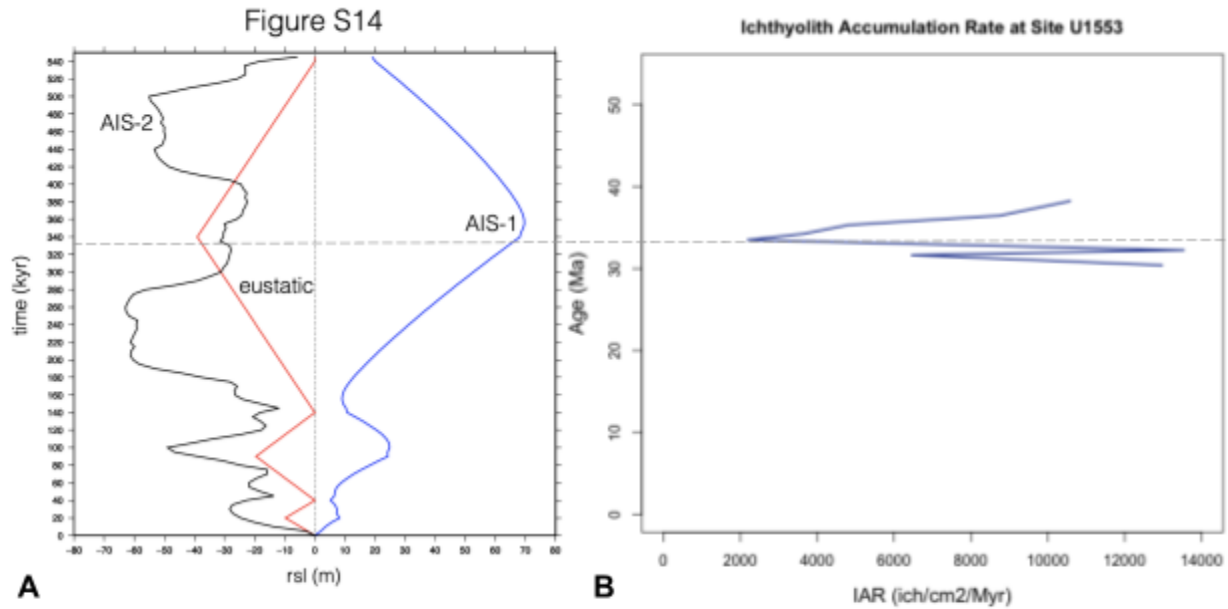
Figure 10: A. Figure S14 from Galeotti et al. 2016 [39] showing Antarctic Sea Ice extent as a function of sea level fall (eustatic in red, projected relative in blue (model AIS-1) and black (model AIS-2); B. IAR at Site U1553, plotted over the same time scale in order to draw comparison. EOB is shown with a grey dashed line

Global

This dataset joins existing ichthyolith data from across the globe. There is a high degree of variability observed across sites, showing that the factors influencing pelagic fish populations were likely different at different sites, implying strong local drivers for fish populations at the EOT. Using ichthyoliths as a proxy is a relatively new method, so trends are still being established as more research is done.

Site U1553 is characterized by its high Southern latitude and proximity to land compared to the other sites, benefitting from upwelling and potentially terrestrial nutrient runoff[15–17]. Fish productivity at Site U1553 is much higher than other sites before and after the EOT, but declines briefly across the interval to levels closer to those observed at other sites. Only Site U1406, which, similarly to IODP Site U1553, is located close to land at a high (Northern) latitude, experiences nearly as much variability across the interval.

Productivity at Site U1553 is double that of Site U1406 both before and after the EOT, confirming that U1553 was a highly productive site, in line with its shallow water depth and proximity to known upwelling regions today. The nutrient cycling associated with upwelling allows for larger populations to be sustained in one general location. The establishment of the ACC would have contributed to increased upwelling at Site U1553 due to more water moving through the area, which would have in turn contributed to an increase in primary productivity that could have supported the rebound of fish populations.
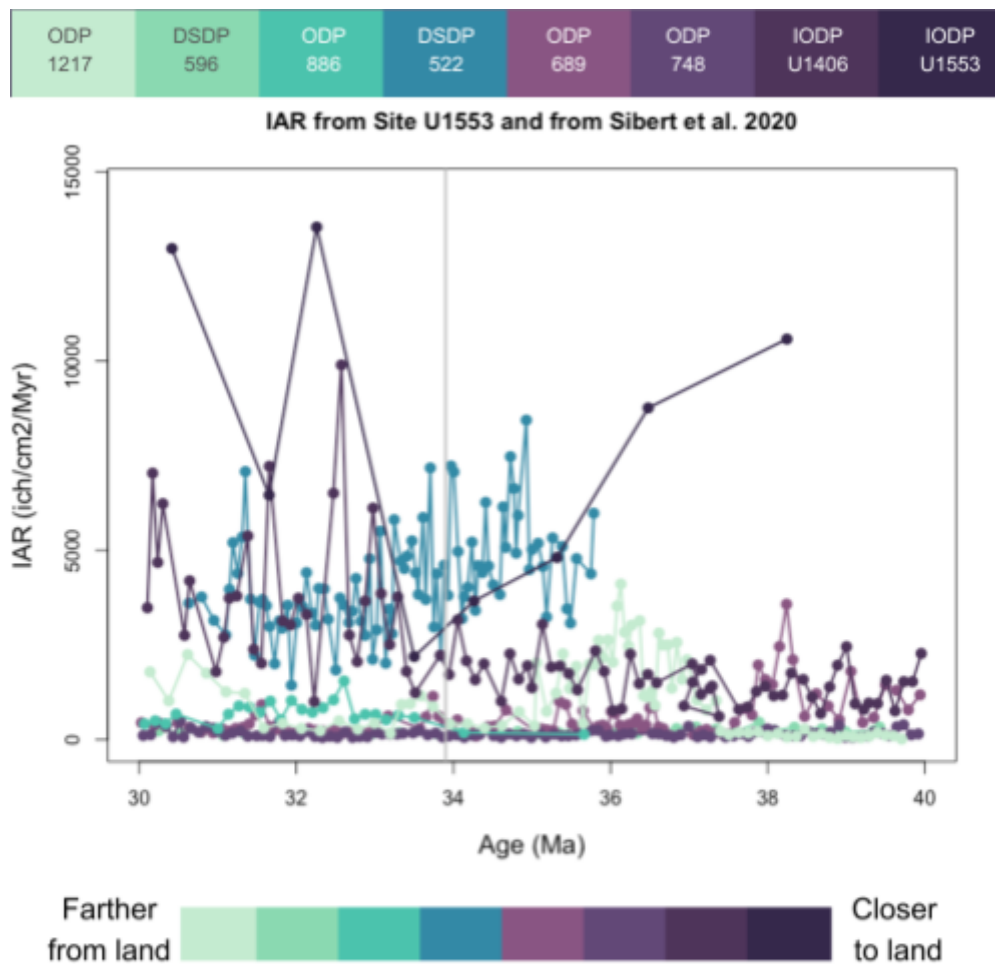

Figure 11: Comparison of Site U1553 data with existing global sites[50]. Sites were color-coded by approximated distances from land. Reconstructed E-O site locations can be seen in Fig. 2 (Background).

Site U1553 appears to have the largest relative change in fish productivity around the EOT compared to the other sites, which do not show similar transient changes in IAR. A higher temporal resolution through the processing of more samples from this site would help improve the understanding of the patterns at Site U1553 by making the results more statistically significant.
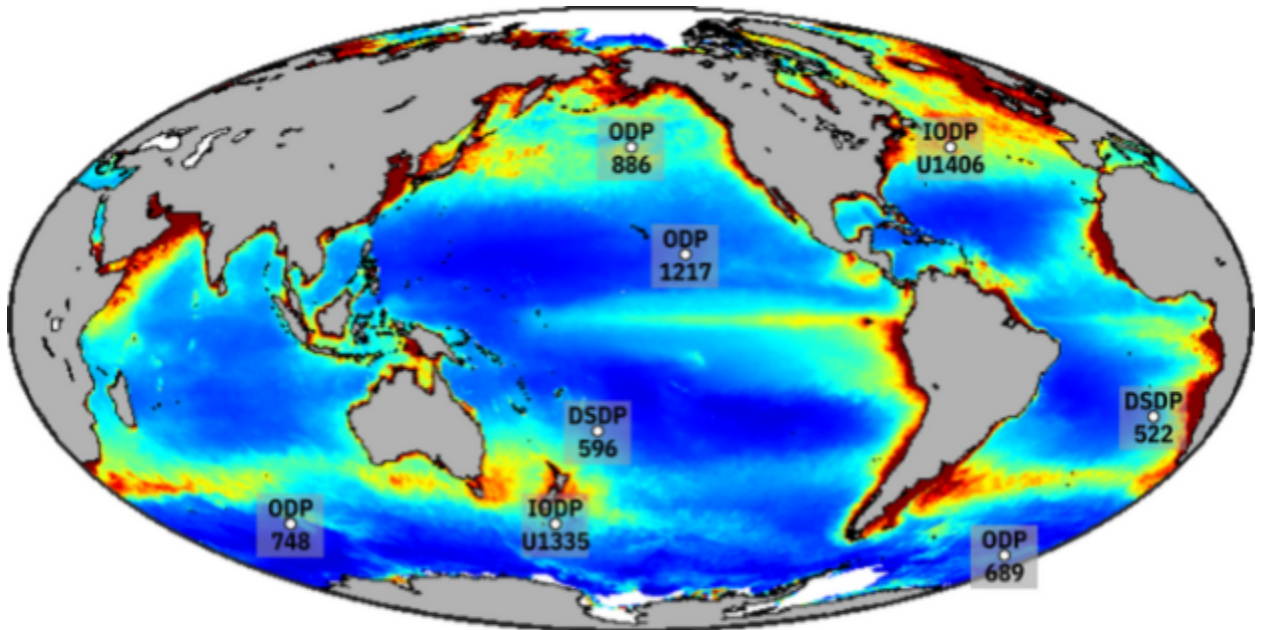

Figure 12: Base map from Oregon State [57] showing annual average net primary productivity in 2020; Site locations added by self, site coordinate data taken from proceedings reports for each (cited in Supplements section).

Records of phytoplanktonic and benthic communities and sedimentary opal (formed from the deposition of siliceous organisms such as diatoms[56]) suggest higher primary production in the high southern latitudes through the middle Eocene and another increase near the EOT. This is matched by records of productivity increases in the South and equatorial Atlantic, Northwestern Australia, and sites close to continental margins[47,57]. This contributes to expectations of higher fish biomass across the EOT at land-proximate sites, and increased primary productivity could be a mechanism behind the observed rebound in pelagic fish populations observed after 33.9 Ma.

Conclusion & Future Directions

Pelagic fish populations at IODP Site U1553 appear to be negatively affected by the major oceanographic changes at the EOT including a decline in ocean temperature, increased ice volume, and increased circulation. However, the decline in fish production was transient, suggesting that, when given time and the conditions to adapt, fish populationsare resilient. Interpreted through IAR, fish productivity at Site U1553 does not follow the same productivity trends as open-ocean sites across the same interval[50]. This site would benefit from further data collection across the interval to establish more statistically significant trends.

Additional biodiversity information about the EOT could improve understanding of the drivers of fish population changes (for example. a shift from temperature-control versus salinity- or nutrient-control of an ecosystem would likely be reflected by a shift in fish diversity as different plankton prey will be consumed by different fish species). This could be tested by tracking changes in tooth morphologies throughout the record. Initially, the scope of this project was intended to include tracking morphological data for each of the samples. Unfortunately, this aspect of the project was abandoned due to time constraints, but would be an important expansion of this dataset, as would the processing and picking of the remaining samples across this interval from the site. Additionally, as more IODP Sites are drilled, more ichthyolith data from the Eocene-Oligocene can be collected, potentially increasing understanding of fish productivity patterns across the interval.

The implications for modern-day climate change are ones of immediate action and long-term hope. The results of this thesis show that fish populations have the capacity to be resilient, but must be given the conditions to succeed. Beyond the appeal of natural biodiversity and preservation of the natural world, the oceans provide food and livelihoods for much of the

world's population. As our understanding of modern climate change and of the sensitivity to change of marine ecosystems improves, our work to preserve and maintain these ecosystems must improve as well.

References

1. Hutchinson, D. K. *et al.* The Eocene–Oligocene transition: a review of marine and terrestrial proxy data, models and model–data comparisons. *Clim. Past* **17**, 269–315 (2021).
2. Lear, C. H., Bailey, T. R., Pearson, P. N., Coxall, H. K. & Rosenthal, Y. Cooling and ice growth across the Eocene-Oligocene transition. *Geology* **36**, 251–254 (2008).
3. Inglis, G. N. *et al.* Descent toward the Icehouse: Eocene sea surface cooling inferred from GDGT distributions. *Paleoceanography* **30**, 1000–1020 (2015).
4. Liu, Z. *et al.* Global Cooling During the Eocene-Oligocene Climate Transition. *Science* **323**, 1187–1190 (2009).
5. Hren, M. T. *et al.* Terrestrial cooling in Northern Europe during the Eocene–Oligocene transition. *Proc. Natl. Acad. Sci.* **110**, 7562–7567 (2013).
6. Zachos, J. C. & Kump, L. R. Carbon cycle feedbacks and the initiation of Antarctic glaciation in the earliest Oligocene. *Glob. Planet. Change* **47**, 51–66 (2005).
7. Bambach, R. K. Phanerozoic Biodiversity Mass Extinctions. *Annu. Rev. Earth Planet. Sci.* **34**, 127–155 (2006).
8. Ivany, L. C., Patterson, W. P. & Lohmann, K. C. Cooler winters as a possible cause of mass extinctions at the Eocene/Oligocene boundary. *Nature* **407**, 887–890 (2000).
9. Hartenberger, J.-L. An Asian Grande Coupure. *Nature* **394**, 321–321 (1998).
10. Meng, J. & McKenna, M. C. Faunal turnovers of Palaeogene mammals from the Mongolian Plateau. *Nature* **394**, 364–367 (1998).
11. Sun, J. *et al.* Synchronous turnover of flora, fauna and climate at the Eocene–Oligocene Boundary in Asia. *Sci. Rep.* **4**, 7463 (2014).
12. Alroy, J. Constant extinction, constrained diversification, and uncoordinated stasis in North American mammals. *Palaeogeogr. Palaeoclimatol. Palaeoecol.* **127**, 285–311 (1996).
13. Seiffert, E. R. Evolution and Extinction of Afro-Arabian Primates Near the Eocene-Oligocene Boundary. *Folia Primatol. (Basel)* **78**, 314–327 (2007).
14. U. Röhl *et al.* Site U1553. *Proc. Int. Ocean Discov. Program* **378**,.
15. Abelson, M., Agnon, A. & Almogi-Labin, A. Indications for control of the Iceland plume on the Eocene–Oligocene "greenhouse–icehouse" climate transition. *Earth Planet. Sci. Lett.* **265**, 33–48 (2008).
16. Davies, R., Cartwright, J., Pike, J. & Line, C. Early Oligocene initiation of North Atlantic Deep Water formation. *Nature* **410**, 917–920 (2001).
17. Huber, M. & Nof, D. The ocean circulation in the southern hemisphere and its climatic impacts in the Eocene. *Palaeogeogr. Palaeoclimatol. Palaeoecol.* **231**, 9–28 (2006).
18. Munkittrick, K. R. & Dixon, D. G. A holistic approach to ecosystem health assessment using fish population characteristics. *Hydrobiologia* **188**, 123–135 (1989).
19. Rapport, D. J., Costanza, R. & McMichael, A. J. Assessing ecosystem health. *Trends Ecol. Evol.* **13**, 397–402 (1998).
20. *The State of World Fisheries and Aquaculture. Sustainability in action.* 244

https://doi.org/10.4060/ca9229en (2020).

21. Andrews, N. *et al.* Oil, fisheries and coastal communities: A review of impacts on the environment, livelihoods, space and governance. *Energy Res. Soc. Sci.* **75**, 102009 (2021).

22. Brunner, E. J., Jones, P. J. S., Friel, S. & Bartley, M. Fish, human health and marine ecosystem health: policies in collision. *Int. J. Epidemiol.* **38**, 93–100 (2009).

23. Wilson, D. S. *et al.* Antarctic topography at the Eocene–Oligocene boundary. *Palaeogeogr. Palaeoclimatol. Palaeoecol.* **335–336**, 24–34 (2012).

24. Bohaty, S. M., Zachos, J. C. & Delaney, M. L. Foraminiferal Mg/Ca evidence for Southern Ocean cooling across the Eocene–Oligocene transition. *Earth Planet. Sci. Lett.* **317–318**, 251–261 (2012).

25. Hodel, F. *et al.* Eocene-Oligocene southwest Pacific Ocean paleoceanography new insights from foraminifera chemistry (DSDP site 277, Campbell Plateau). *Front. Earth Sci.* **10**, :998237 (2022).

26. Zanazzi, A., Kohn, M. J., MacFadden, B. J. & Terry, D. O. Large temperature drop across the Eocene–Oligocene transition in central North America. *Nature* **445**, 639–642 (2007).

27. Berggren, W. A. A Cenozoic time-scale — some implications for regional geology and paleobiogeography. *Lethaia* **5**, 195–215 (1972).

28. Gradstein, F. M., Ogg, J. G., Schmitz, M. & Ogg, G. *The Geologic Time Scale 2012*. (Elsevier, 2012).

29. Walker, J. D. & Geissman, J. W. GSA 2020. *Geol. Soc. Am.* (2022) doi:10.1130/2022.CTS006C.

30. Pagani, M., Zachos, J. C., Freeman, K. H., Tipple, B. & Bohaty, S. Marked Decline in Atmospheric Carbon Dioxide Concentrations during the Paleogene. *Science* **309**, 600–603 (2005).

31. DeConto, R. M. & Pollard, D. Rapid Cenozoic glaciation of Antarctica induced by declining atmospheric CO2. *Nature* **421**, 245–249 (2003).

32. Schouten, S., Hopmans, E. C., Schefuß, E. & Sinninghe Damsté, J. S. Distributional variations in marine crenarchaeotal membrane lipids: a new tool for reconstructing ancient sea water temperatures? *Earth Planet. Sci. Lett.* **204**, 265–274 (2002).

33. Meckler, A. N. *et al.* Cenozoic evolution of deep ocean temperature from clumped isotope thermometry. *Science* **377**, 86–90 (2022).

34. Alvarez, W., Asaro, F., Michel, H. V. & Alvarez, L. W. Iridium Anomaly Approximately Synchronous with Terminal Eocene Extinctions. *Science* **216**, 886–888 (1982).

35. Alvarez, L. W., Alvarez, W., Asaro, F. & Michel, H. V. Extraterrestrial Cause for the Cretaceous-Tertiary Extinction. *Science* **208**, 1095–1108 (1980).

36. Corliss, B. H. *et al.* The Eocene/Oligocene Boundary Event in the Deep Sea. *Science* **226**, 806–810 (1984).

37. The Ocean's Carbon Balance. https://earthobservatory.nasa.gov/features/OceanCarbon (2008).

38. Pekar, S. F., Christie-Blick, N., Kominz, M. A. & Miller, K. G. Calibration between eustatic

estimates from backstripping and oxygen isotopic records for the Oligocene. *Geology* **30**, 903–906 (2002).

39. Galeotti, S. *et al.* Antarctic Ice Sheet variability across the Eocene-Oligocene boundary climate transition. *Science* **352**, 76–80 (2016).

40. Sarkar, S. *et al.* Late Eocene onset of the Proto-Antarctic Circumpolar Current. *Sci. Rep.* **9**, 10125 (2019).

41. Diester-Haass, L. & Zahn, R. Paleoproductivity increase at the Eocene–Oligocene climatic transition: ODP/DSDP sites 763 and 592. *Palaeogeogr. Palaeoclimatol. Palaeoecol.* **172**, 153–170 (2001).

42. Legendre, S. *et al.* Evolution de la diversite des faunes de Mammiferes d'Europe occidentale au Paleogene (MP 11 a MP 30). *Bull. Société Géologique Fr.* **162**, 867–874 (1991).

43. Zhang, R., Kravchinsky, V. A. & Yue, L. Link between global cooling and mammalian transformation across the Eocene–Oligocene boundary in the continental interior of Asia. *Int. J. Earth Sci.* **101**, 2193–2200 (2012).

44. Sun, J. & Windley, B. F. Onset of aridification by 34 Ma across the Eocene-Oligocene transition in Central Asia. *Geology* **43**, 1015–1018 (2015).

45. How the ocean shapes weather and climate. *World Meteorological Association* https://public.wmo.int/en/our-mandate/focus-areas/oceans/weather-and-climate (2021).

46. Sigman, D. M. & Hain, M. P. The Biological Productivity of the Ocean. *Nature Education* https://www.nature.com/scitable/knowledge/library/the-biological-productivity-of-the-ocean-70631104/.

47. Coxall, H. K. & Wilson, P. A. Early Oligocene glaciation and productivity in the eastern equatorial Pacific: Insights into global carbon cycling. *Paleoceanography* **26**, (2011).

48. Egan, K. E., Rickaby, R. E. M., Hendry, K. R. & Halliday, A. N. Opening the gateways for diatoms primes Earth for Antarctic glaciation. *Earth Planet. Sci. Lett.* **375**, 34–43 (2013).

49. Berger, W. H. Cenozoic cooling, Antarctic nutrient pump, and the evolution of whales. *Deep Sea Res. Part II Top. Stud. Oceanogr.* **54**, 2399–2421 (2007).

50. Sibert, E. C., Zill, M. E., Frigyik, E. T. & Norris, R. D. No state change in pelagic fish production and biodiversity during the Eocene–Oligocene transition. *Nat. Geosci.* **13**, 238–242 (2020).

51. Sibert, E. C., Cramer, K. L., Hastings, P. A. & Norris, R. D. Methods for isolation and quantification of microfossil fish teeth and elasmobranch dermal denticles (ichthyoliths) from marine sediments. *Palaeontol. Electron.* **20**, 1–14 (2017).

52. LST Heavy Liquid for density separations. *Central Chemical Consulting* https://www.chem.com.au/heavy_liquid.html.

53. Britten, G. L. & Sibert, E. C. Enhanced fish production during a period of extreme global warmth. *Nat. Commun.* **11**, 5636 (2020).

54. Keller, G. Biochronology and paleoclimatic implications of Middle Eocene to Oligocene planktic foraminiferal faunas. *Mar. Micropaleontol.* **7**, 463–486 (1983).

55. Hollis, C. J. *et al.* The Paleocene–Eocene Thermal Maximum at DSDP Site 277, Campbell

Plateau, southern Pacific Ocean. *Clim. Past* **11**, 1009–1025 (2015).

56. Mortlock, R. A. & Froelich, P. N. A simple method for the rapid determination of biogenic opal in pelagic marine sediments. *Deep Sea Res. Part Oceanogr. Res. Pap.* **36**, 1415–1426 (1989).

57. Ocean Productivity: Annual Average NPP. *Ocean Productivity: Oregon State* http://orca.science.oregonstate.edu/npp.annual.comparison.modis.php?year=2020.

Acknowledgements

I am immensely grateful for the people and communities who have helped me learn and grow throughout my time at Yale and before. This thesis would not be possible without the unending patience and commitment to teaching of my advisor, Dr. Elizabeth Sibert. Dr. Pincelli Hull made me feel so welcome in her lab. Together, they helped me navigate the worlds of laboratory science and marine paleobiology. I appreciate the ongoing support (occasionally in the form of a snack) of other members of the Hull Lab, E&PS graduate students Maoli Vizcaino and Elly Goetz.

More broadly, I owe much to the people who helped me get to (and through) my time at Yale. First, Noreen and David Henig, for fostering a curiosity and desire to learn from childhood. Next, the swimming coaches at and before Yale who cultivated the work ethic I needed to succeed and provided support on the challenging days. These include, but are not limited to, Jim Henry, Kyle Schack, Connor Beaulieu, Molly Chamberlain, Dana Kirk, Bruce Smith, and Scott Shea. I owe a special thank-you to my peers including my friends (including the CCEs and 2023 PCs) and my teammates on Yale Swim & Dive and Palo Alto Stanford Aquatics who kept my love for the water –and all the things that live in it– alive.

Supplementary Figures & Data

Data Table 1

Ser #	Hole	C#	CT	Sec	Half	Top	Bot.	Age*	Sed Rt	IAR	Lrg D	Lrg T	Md D	Md T	Sm D	Sm T	Tot. Ich.
33	B	12	H	2	W	97	101	30.4170166	3.275438596	12974.24301	0	8	0	36	0	147	191
37	E	16	H	2	W	94	98	31.65447046	2.792676736	6460.735212	0	10	0	55	0	44	109
39	A	18	H	5	W	32	36	32.25947312	1.917346939	13539.74897	2	21	0	73	0	207	303
43	A	20	H	5	W	10	14	33.50109475	1.408255529	2194.301871	1	7	0	10	0	54	72
45	B	20	X	3	W	3	7	34.26210646	1.187892377	3660.864753	0	24	0	15	0	73	112
49	B	22	X	1	W	86	93	35.31902039	1.187892377	4812.421575	3	27	0	50	0	80	160
54	A	26	X	1	W	46	50	36.47897872	1.19874031	8762.704487	1	7	0	42	0	147	197
57	B	27	X	1	W	1	5	38.24449887	4.190526316	10582.15748	2	5	2	27	0	44	80

Notes:
Ser # = Serial Number
C# = Core Number
CT = Core Type
Sect = Section
Top and Bot. (Bottom) in cm
Age is a linear interpolation, in Ma.
Sed. Rt. (Sedimentation Rate) in cm/Myr
IAR in ich/cm^2/Myr
Lrg = Large (106-150μm)
Md = Medium (63-106μm)
Sm = Small (38-63μm)
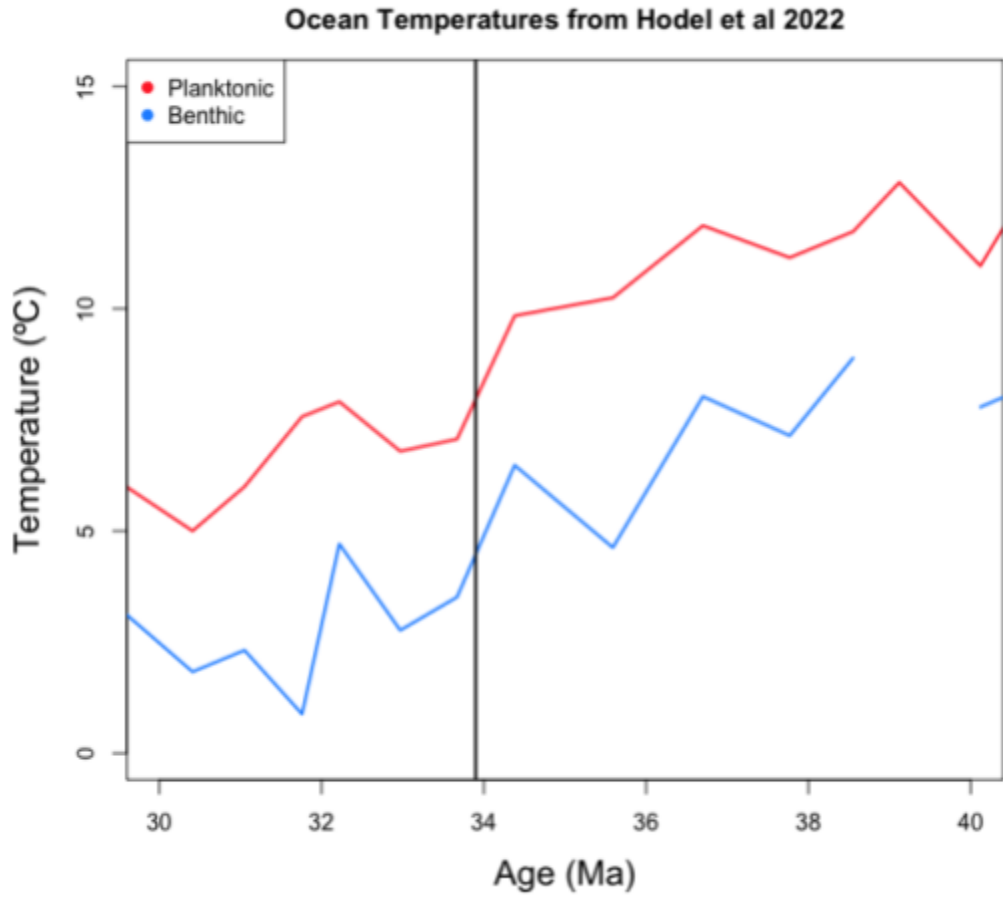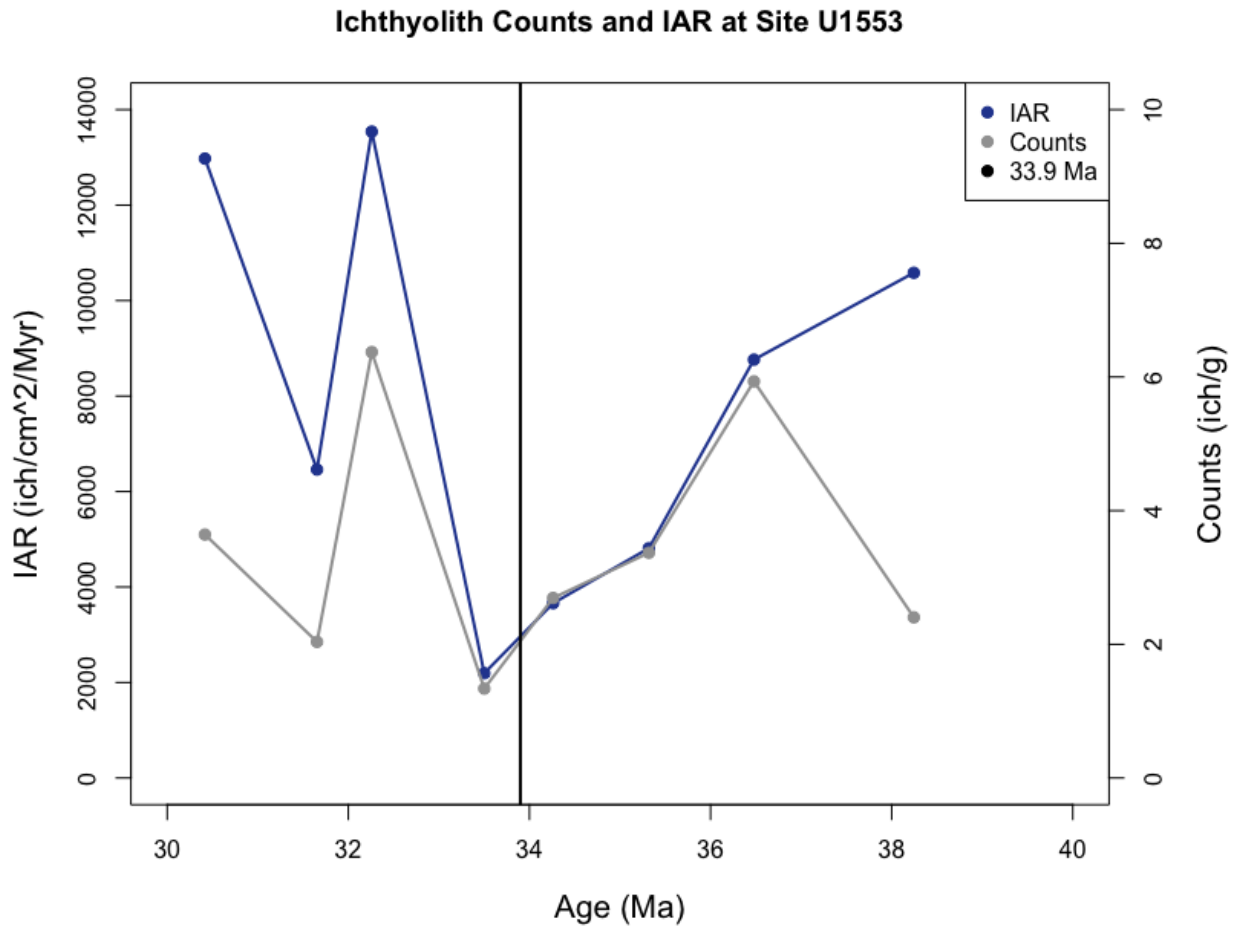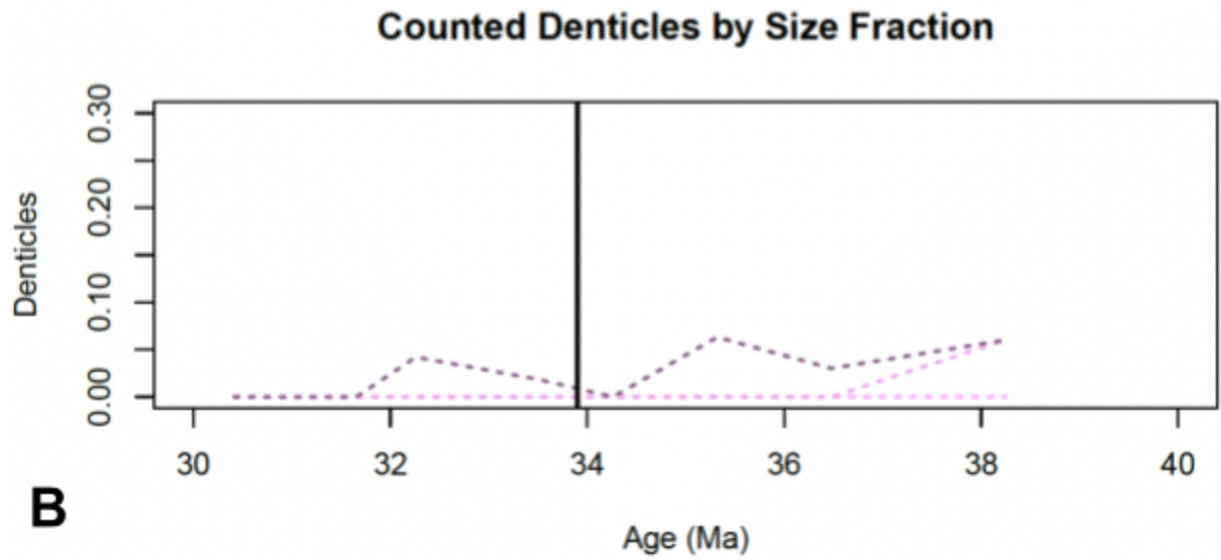D = Denticles; T = Teeth
Tot. Ich = Total Ichthyoliths

Figure 1

Ocean Temperatures from Hodel et al 2022

Figure 2

Figure 6

Ichthyolith Counts and IAR at Site U1553

Figure 7

Ichthyolith Counts by Size Fraction

A

Small Teeth — Medium Teeth — Large Teeth ···· Small Denticles ···· Medium Denticles ···· Large Denticles

Counted Denticles by Size Fraction

B

Figure 8

Figure 9

Site U1553 IAR and Pelagic Ocean Temperatures
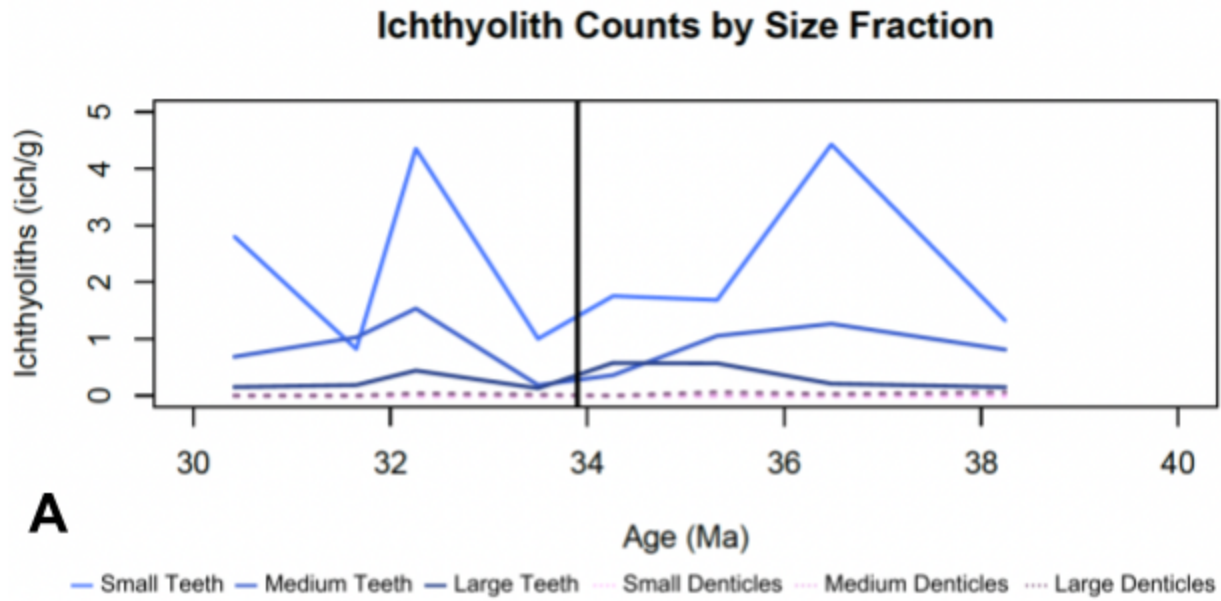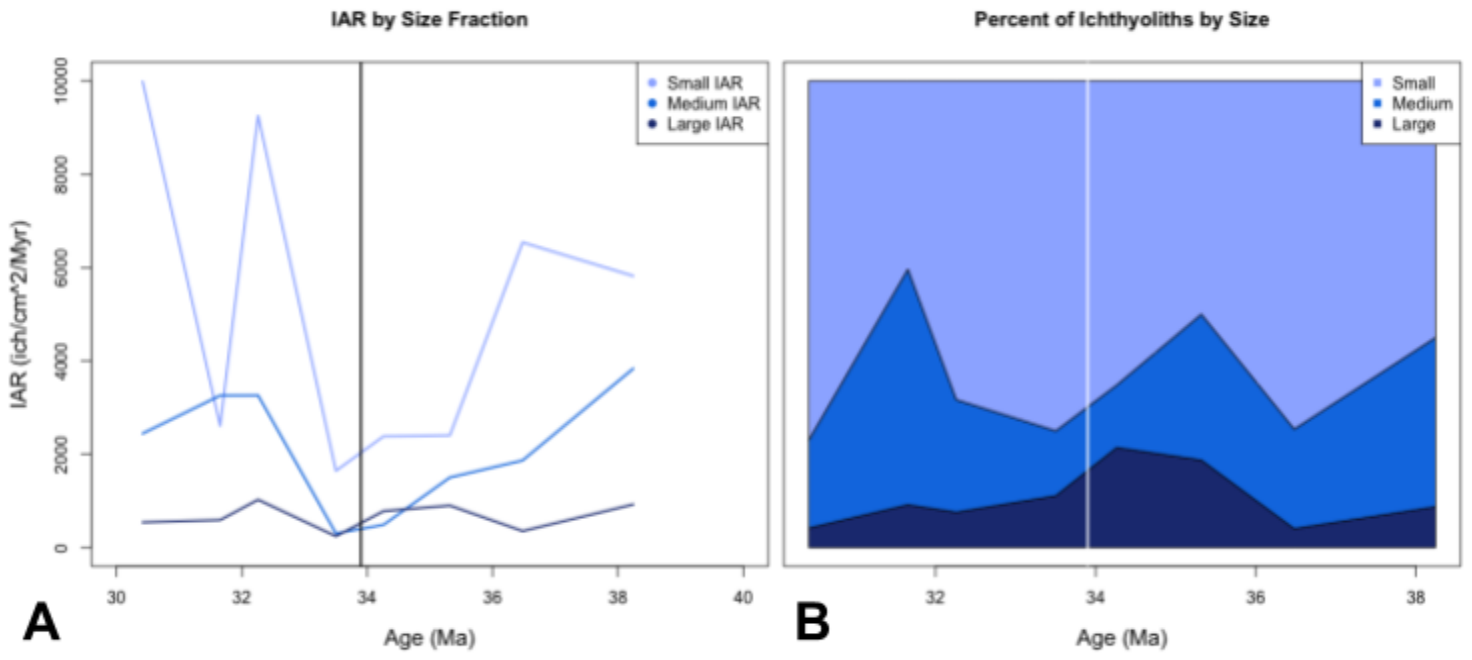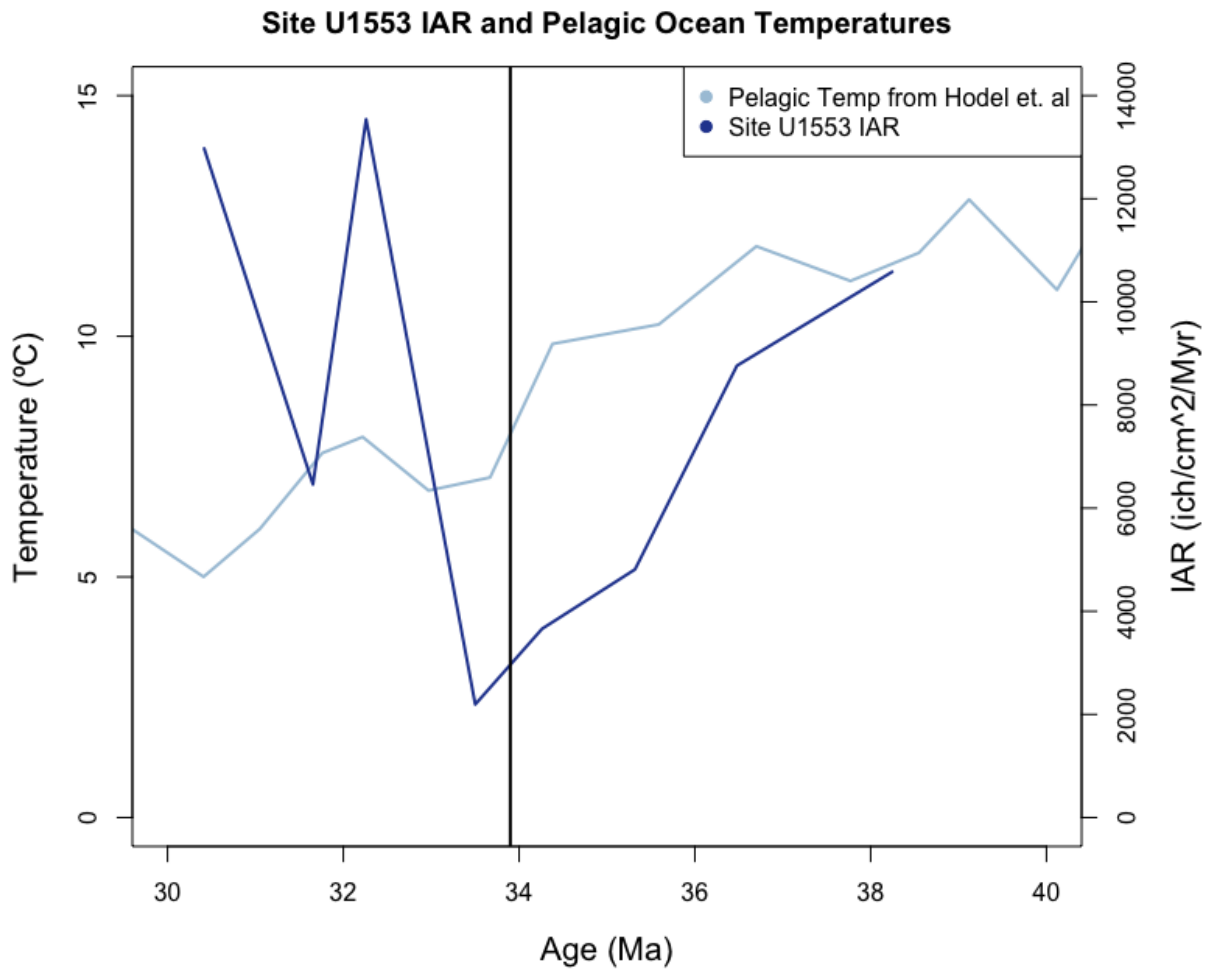
Figure 10 - IAR and Ice Volume

Figure 11 - Global IARs

ODP 1217	DSDP 596	ODP 886	DSDP 522	ODP 689	ODP 748	IODP U1406	IODP U1553
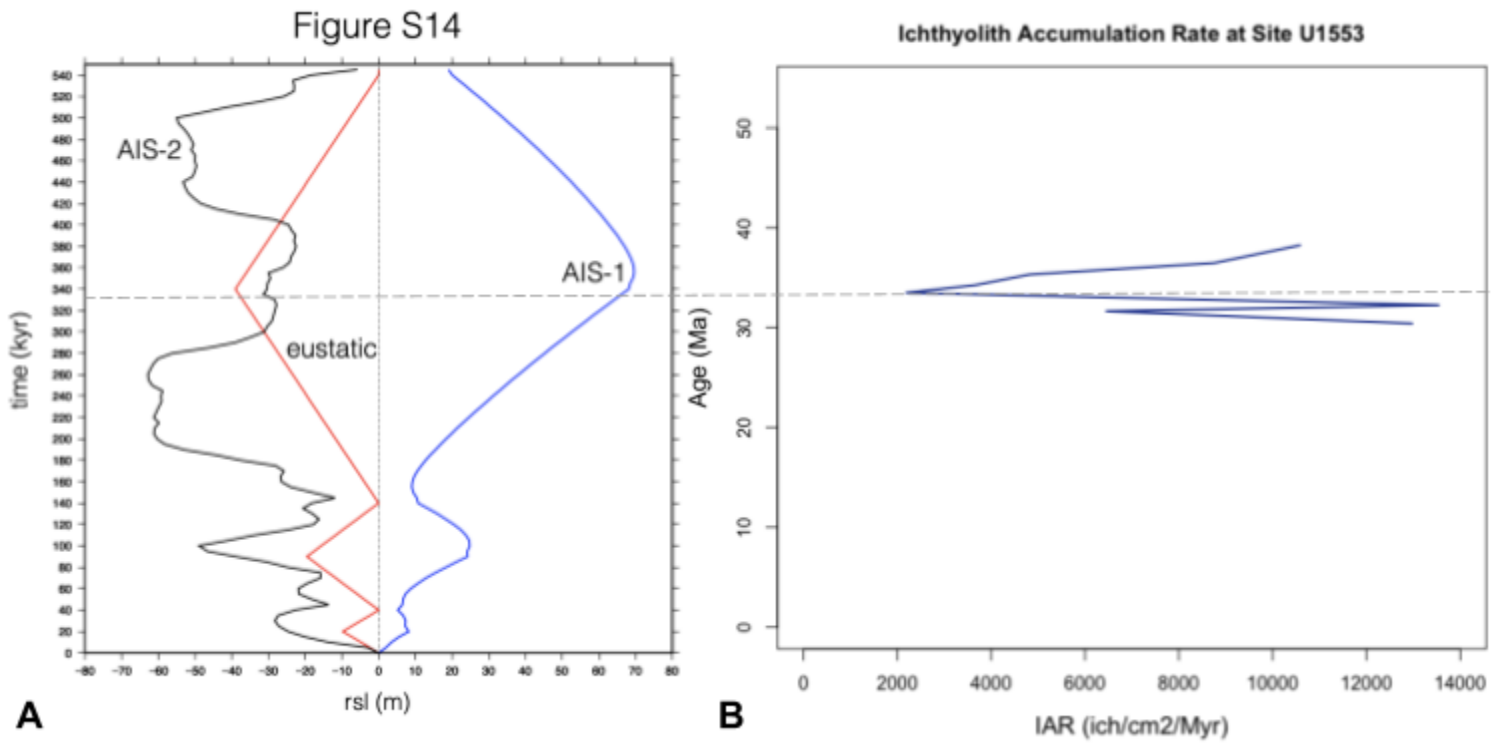
IAR from Site U1553 and from Sibert et al. 2020

Farther from land — Closer to land
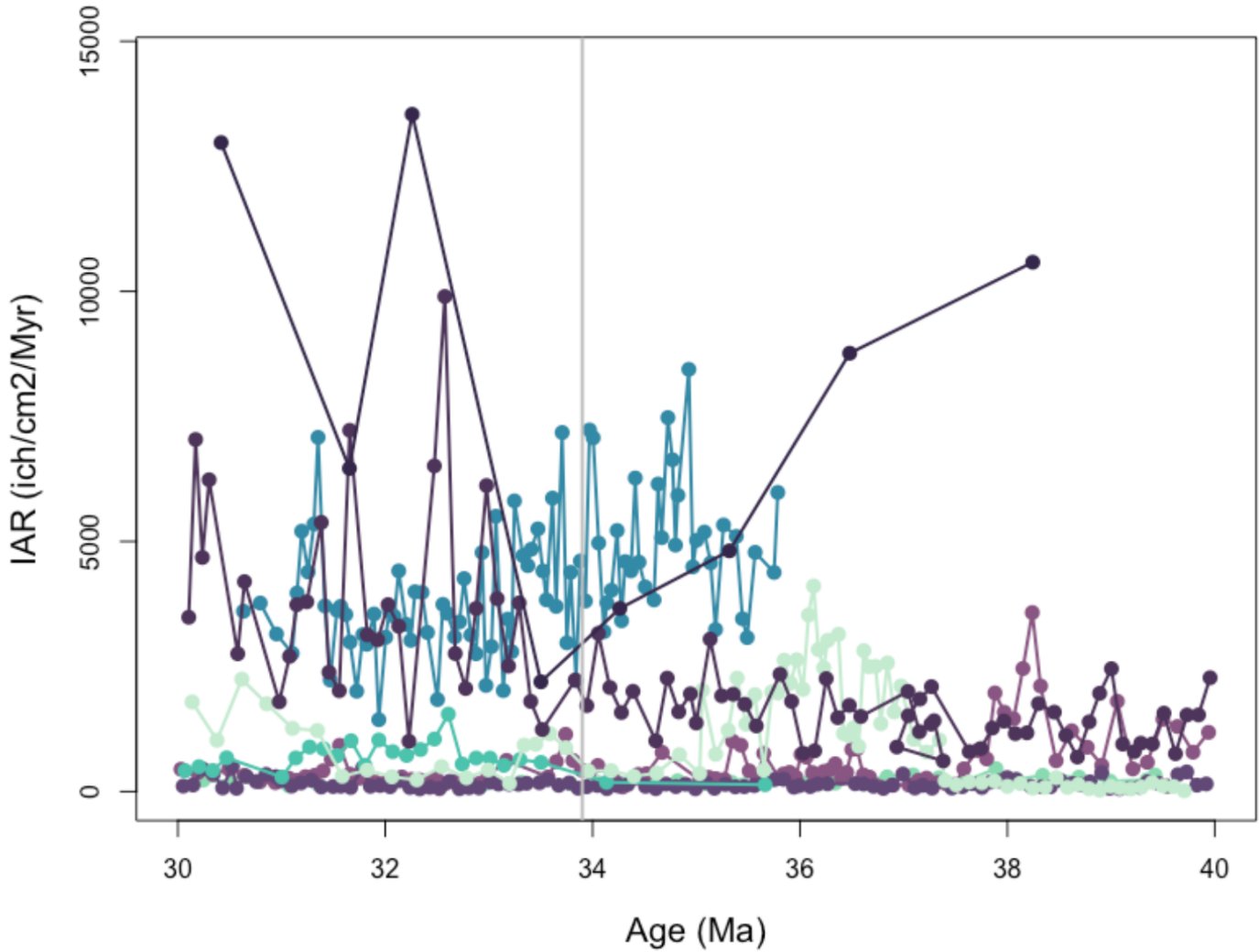
Figure 12 - Productivity Map
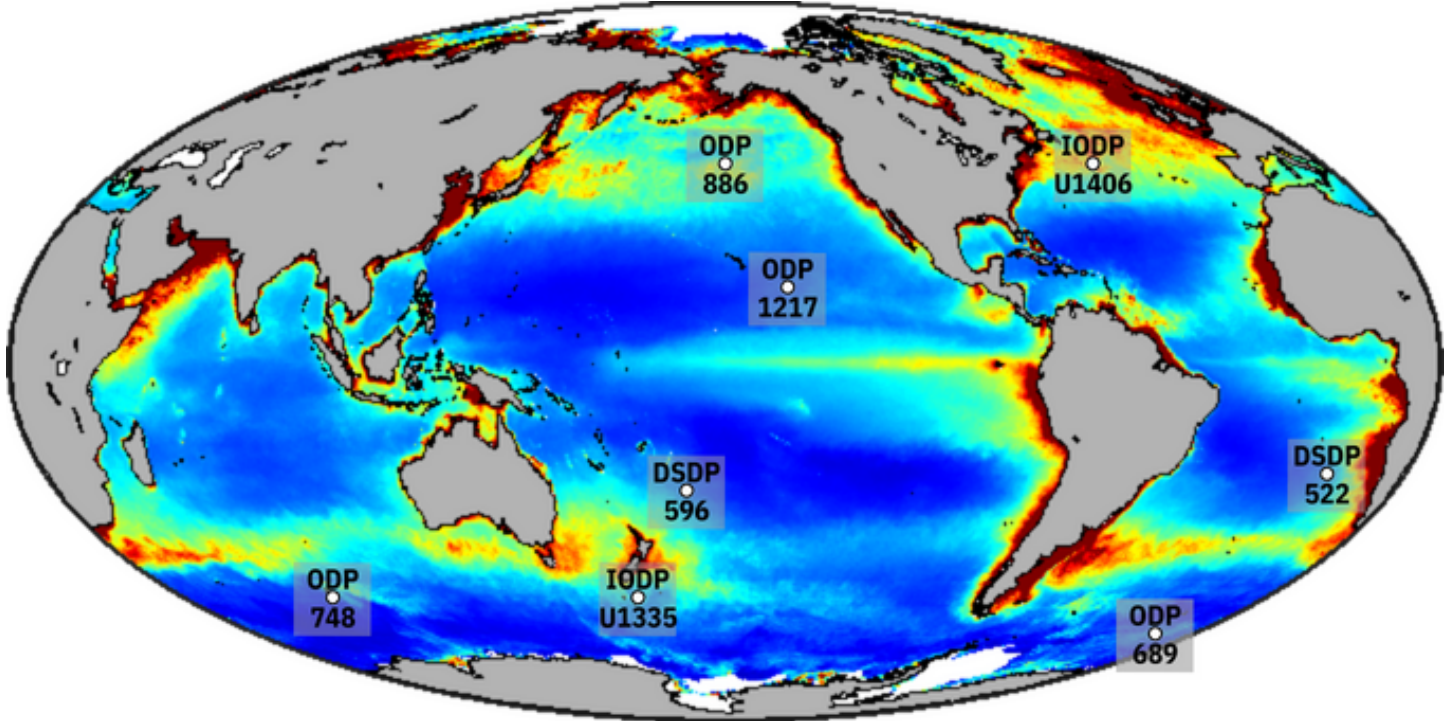
Modern Site Location Sources

Barker, Peter F., et al. "Site 689." *Proceedings of the Ocean Drilling Program, Part A: Initial Reports* Vol. 113 (1988): p.89-181. doi:10.2973/odp.proc.ir.113.106.1988

Hsü, Kenneth J., et al. "Site 522." *Initial Reports of the Deep Sea Drilling Project* Vol. 73 (1984): p.187-270. doi:10.2973/dsdp.proc.73.105.1984

Lyle, Mitchell W., et al. "Site 1217." *Proc. of the Ocean Drilling Program, Part A: Initial Reports* Vol. 199 (2002): 64p.. doi:10.2973/odp.proc.ir.199.110.2002

Menard, H. William, et al. "Site 596; Hydraulic Piston Coring in an Area of Low Surface Productivity in the Southwest Pacific." *Initial Reports of the Deep Sea Drilling Project* Vol. 91 (1987): p.245-267. doi:10.2973/dsdp.proc.91.103.1987

Norris, Richard D., et al. "Site U1406." *Proceedings of the Integrated Ocean Drilling Program (Online)* Vol. 342 (2014): 99p. doi:10.2204/iodp.proc.342.107.2014

Palike, Heiko, et al. "Site U1335." *Proceedings of the Integrated Ocean Drilling Program* Vol. 320 (2010) doi:10.2204/iodp.proc.320321.107.2010

Rea, David K., et al. "Sites 885/886." *Proceedings of the Ocean Drilling Program, Part A: Initial Reports* Vol. 145 (1993): p.303-334. doi:10.2973/odp.proc.ir.145.109.1993

Schlich, Roland, et al. "Site 748." *Proceedings of the Ocean Drilling Program, Part A: Initial Reports* Vol. 120 (1989): p.157-235. doi:10.2973/odp.proc.ir.120.110.1989